A Tensor Completion-Based Selection Method of a Single Data Collection Point for Multiple Shelters in a UAV Enabled Disaster Recovery Network

Azusa Danjo*† Shinsuke Hara*, Takahiro Matsuda‡ and Fumie Ono§
*Graduate School of Engineering, Osaka City University
3-3-138 Sugimoto, Sumiyoshi-ku, Osaka 558–8585, Japan
Email: {danjo@c., hara@}info.eng.osaka-cu.ac.jp
†DAIHEN Corporation
2-1-11 Tagawa, Yodogawa-ku, Osaka 532–8512, Japan
‡Graduate School of Systems Design, Tokyo Metropolitan University
6-6 Asahiga-oka, Hino, Tokyo, 191–0065, Japan
Email: takahiro.m@tmu.ac.jp
§National Institute of Information and Communications Technology
3-4 Hikarino-Oka, Yokosuka, Kanagawa, 239–0847, Japan
Email: fumie@nict.go.jp

***Abstract*—In this paper, we propose a method for selecting a single data collection point for an Unmanned Aerial Vehicle (UAV)-enabled disaster recovery network where UAVs need to collect messages from refugees while hovering above multiple shelters. Just by sensing the Received Signal Strengths (RSSs) for the wireless signals transmitted from multiple shelters at *fewer randomly-selected* points in the three-dimensional (3D) region above a disaster-hit area, through a tensor completion, the proposed method reconstructs full RSS maps for the multiple shelters in the entire 3D region, and selects a single data collection point using the reconstructed RSS maps where UAVs can collect messages from them more quickly and more energy-efficiently. The experimental results reveal that by sensing RSSs in 25% of a 3D region, the proposed method can collect messages from three transmitters using a shorter route of UAV in a shorter message collection time.**

Keywords–Unmanned Aerial Vehicle; Received Signal Strength; Tensor Completion.

I. INTRODUCTION

When a large-scale disaster causes catastrophic damage to infrastructure and lifeline, such as roads, buildings, water, gas, electric power and information networks, a lot of people are dead and forced to live as refugees in shelters. The primary concern of refugees is to let them know their families' safety and let their families know their safety, therefore, before the recovery of terrestrial information network, it is essential to quickly construct a temporary information network in the disaster-hit area.

Since Unmanned Aerial Vehicles (UAVs) can quickly fly anywhere in the sky, they are promised to play an essential in it, where UAVs, which are equipped with wireless communication tools, visit to collect messages from refugees while hovering above shelters [1].

In the usage of UAVs, there is one serious problem, and that is the operation time is severely limited even thanks to the current battery technology, such as typically 20-40 minutes and the energy consumption by flying and hovering is dominant. Therefore, when a region in a disaster-hit area is assigned to a UAV, if there are many shelters to visit in the region, it may be prohibitive for the UAV to visit all the shelters. In this case, it should be better for the UAV to collect messages from multiple shelters at *a single* point where the UAV can receive the wireless signals from them simultaneously in better channel conditions. This is also effective for enlarging the size of region assigned to a UAV.

Let us assume that a disaster-hit area has been divided into many three-dimensional (3D) regions. The quality of wireless channel is proportional to Received Signal Strength (RSS), so we believe it reasonable to divide the UAV operation into two stages, such as RSS sensing stage and message collection stage. In the RSS sensing stage, a UAV visits many points in a 3D region assigned to it, and it senses the RSSs for multiple shelters there. Then, we select the one out of the visited points where the RSSs can be larger for the multiple shelters. In the message collection stage, a single point has been selected for each region in the disaster-hit area, so a single or multiple UAVs can visit all the points according to the route solved as a vehicle routing problem (VRP) [2]. Note that how to apply the VRP for the UAV route planning is out of the scope of this paper.

In the RSS sensing stage, there is one more serious problem, and that is wireless channel condition is affected by the distribution of surrounding buildings in urban areas, so even for a single shelter, it is difficult to find a good point where the condition is better for the shelter. Furthermore, if the 3D region is huge, it may be also prohibitive for the UAV to fly fully in the entire 3D region. Therefore, it is mandatory to develop an efficient method to select a single message collection point even for a huge disaster-hit region.

In this paper, by dealing with the 3D-RSS spatial distribution (MAP) as a 3D tensor, we propose a tensor completion-based selection method of a single data collection point for multiple shelters. The use of UAV has been well discussed in disaster recovery scenarios; a UAV-assisted network as a substitute for terrestrial information communication network [3], image collection [4], rescue [5] and so on. However, there have been no works which try to select message collection points in a UAV-enabled disaster recovery network. VRP is

 ISBN: 978-1-61208-769-6

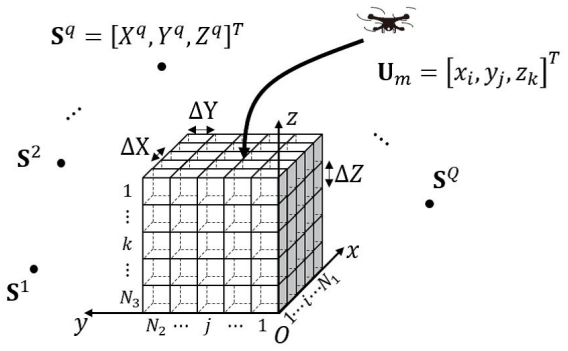

Figure 1. Layout model.

applied for a UAV delivery problem [6], but it selects delivery points in advance, although there is a lot of freedom in selecting them.

This paper is organized as follows. Section II presents the models and assumptions, and Section III mathematically states the problem. Section IV proposes three methods for selection of the RSS sensing points and collection points of messages, and Section V evaluates the performance of the proposed methods using experimental data. Finally, Section VI concludes the paper.

II. Models and Assumptions

It is assumed that the wireless communication tool between refugees and a UAV is Wi-Fi [7], since it has been widely and commonly used as a Wireless Local Area Network (WLAN) standard over the world. However, since many Wi-Fi communication links do not guarantee communication qualities, a Wi-Fi connection may take a long time, for instance, more than 10 sec [8], and this implies that if refugees independently try to access the access point installed in the UAV hovering above them, the message collection time of the UAV becomes extremely longer. Therefore, it is also assumed that in each shelter, there is a server which has already stored the messages of refugees staying it. When the UAV visits a shelter, the server tries to transmit its stored messages to the UAV by Wi-Fi. In the following, servers are referred to as "transmitters (TXs)," and their stored messages are simply referred to as "data."

A. Layout model

Figure 1 shows the layout model, where there is a 3D region of interest $\mathcal{R}$, Q stationary TXs and a flying UAV. The size of $\mathcal{R}$ is Xm $\times$ Ym $\times$ Zm, and $\mathcal{R}$ is divided into $N_1 \times N_2 \times N_3 = N_v$ voxels with size of ΔXm $\times$ ΔYm $\times$ ΔZm, where N_1, N_2 and N_3 denote the number of voxels dividing $\mathcal{R}$ in the x-axis, y-axis and z-axis directions, respectively. We label the voxels with $l = i + N_1(j-1) + N_1N_2(k-1)$ ($l = 1, 2, \ldots, N_v$, $i = 1, 2, \ldots N_1, j = 1, 2, \ldots N_2, k = 1, 2, \ldots N_3$), define the location of the center of gravity of the $l = i+N_1(j-1)+N_1N_2(k-1)$-th voxel as $\mathbf{V}_l = [x_i, y_j, z_k]^T$, and define the set of all $\mathbf{V}_l s$ as $\mathcal{V} = \{\mathbf{V}_1, \mathbf{V}_2, \ldots, \mathbf{V}_{N_v}\}$. In addition, Q TXs are located at the outsides of $\mathcal{R}$ and we define the location of the q-th TX as $\mathbf{S}^q = [X^q, Y^q, Z^q]^T$ ($q = 1, 2, \ldots, Q$).

The UAV visits the centers of gravity of voxels to sense RSSs for Q TXs. We define the location of the m-th visit of UAV as $\mathbf{U}_m$ ($m = 1, 2, \ldots, M$), the set of all $\mathbf{U}_m$s as $\mathcal{U} = \{\mathbf{U}_1, \mathbf{U}_2, \ldots, \mathbf{U}_M\}$ and the sensing rate as $B_{sense} = M/N_v$.

B. Route model

In the RSS sensing stage, a realistic way is to visit and sense RSSs only at fewer part of the voxels along a predetermined route Ω in $\mathcal{R}$. When the voxels to visit have been selected as $\mathcal{U}$, determining the shortest route for visiting all the voxels is a kind of the 3D Traveling Salesman Problem (TSP), and there have been a lot of solvers for the TSP [9] [10]. In this paper, therefore, we do not care about how to determine the shortest route, namely, the "route" in this paper naturally means the shortest route.

C. Wireless communication model

In the RSS sensing stage, Q TXs transmit their wireless signals for UAV, and UAV tries to receive the wireless signals from all the TXs and sense their RSSs, however, in each visit, UAV cannot always receive the wireless signals from all the Q TXs. We define the probability that UAV can receive the wireless signal from the q-th TX in the m-th visit as C_{rec}, and define the RSS as R^q_m in dBm when it is possible.

On the other hand, in the data collection stage, after a single data collection point has been selected, UAV collects the data from all the TXs while hovering at the selected point. When Wi-Fi is employed between the TXs and UAV, the data transmission rate is an increasing function of RSS [11], for instance, $f(R^q_{\hat{m}})$bps, where $\hat{m}$ is the voxel index for the data collection point and $R^q_{\hat{m}}$ is the RSS for the q-th TX at the data collection point. Therefore, defining the size of data for the q-th TX as D^q bits, its required data collection time is given by

$$T^q_{\hat{m}} = D^q / f(R^q_{\hat{m}}). \tag{1}$$

III. Problem Statement

Selection of a single data collection point is divided into the following two optimization problems.

A. RSS sensing stage

UAV sequentially visits $\mathbf{U}_1, \mathbf{U}_2, \ldots, \mathbf{U}_M$, so defining the route length as L_{route}, the problem is given by

$$\text{find} \quad \mathcal{U} = \{\mathbf{U}_1, \mathbf{U}_2, \ldots, \mathbf{U}_M\} \subseteq \mathcal{V} \tag{2}$$

$$\text{which minimizes} \quad L_{route} = \sum_{m=1}^{M-1} \|\mathbf{U}_{m+1} - \mathbf{U}_m\|. \tag{3}$$

B. Data collection stage

The data collection point, which is included in a subset of $\mathcal{V}$, should minimize the total data collection time, so the problem is given by

$$\text{find} \quad \mathbf{U}_{\hat{m}} \in \text{ a subset of } \mathcal{V} \tag{4}$$

$$\text{which minimizes} \quad T_{total} = \sum_{q=1}^{Q} T^q_{\hat{m}}. \tag{5}$$

At $\mathbf{U}_m$, the dominant factor to determine the total data collection time is the maximum among $T^1_m, T^2_m, \ldots, T^Q_m$, and from (1), the data collection time is a decreasing function

 ISBN: 978-1-61208-769-6

of RSS. Therefore, when $D^1 \approx D^2 \approx \ldots \approx D^Q$, defining R_m^{min} as the minimum of $R_m^1, R_m^2, \ldots, R_m^Q$, this problem is reformulated as

$$\text{find} \quad \mathbf{U}_{\hat{m}} \in \text{ a subset of } \mathcal{V} \tag{6}$$

$$\hat{m} = \arg_m \max \quad \{R_1^{min}, R_2^{min}, \ldots, R_M^{min}\}. \tag{7}$$

Once $\hat{m}$ has been selected, the corresponding voxel label can be identified. For instance, for $\mathbf{U}_{\hat{m}} = [x_{\hat{i}}, y_{\hat{j}}, z_{\hat{k}}]^T$, a distinct voxel label is given by $\hat{l} = \hat{i} + N_1(\hat{j}-1) + N_1N_2(\hat{k}-1)$.

IV. Solutions

We propose the following three methods to solve the problem.

A. Full visits and full RSS sensing

If UAV can visit all the voxels where it senses RSSs for all the TXs, it can select the best data collection point, although the route is maximized:

$$\text{find} \quad \mathbf{U}_{\hat{m}} \in \mathcal{V} \tag{8}$$

$$\hat{m} = \arg_m \max \quad \{R_1^{min}, R_2^{min}, \ldots, R_{N_v}^{min}\}. \tag{9}$$

We refer to this method as the Full Visit/Full RSS Sensing (FV/FS) method. Note that the FV/FS method gives the performance lower-bound.

B. Random visits and random RSS sensing

It is very difficult to select M voxels, which gives the shortest route. Therefore, in this paper, we randomly select M voxels out of N_v voxels.

To formulate the problem of selecting the data collection point, we define the set of visited voxels where UAV can sense RSS for the q-th TX ($q = 1, 2, \ldots, Q$):

$$\mathcal{U}^q = \{\mathbf{U}_m \in \mathcal{U} | m = 1, 2, \ldots, M, R_m^q \text{ exists}\}. \tag{10}$$

Furthermore, we define the set of visited voxels where UAV can sense RSSs for all the Q TXs:

$$\mathcal{U}^{1\cdot 2\cdots Q} = \bigcap_{q=1}^{Q} \mathcal{U}^q. \tag{11}$$

Using (11), this problem is given by

$$\text{find} \quad \mathbf{U}_{\hat{m}} \in \mathcal{U}^{1\cdot 2\cdots Q} \tag{12}$$

$$\hat{m} = \arg_m \max \quad \{R_1^{min}, R_2^{min}, \ldots, R_M^{min}\} \tag{13}$$

where R_m^{min} is replaced by 0 when m is not included in the set of indexes of $\mathcal{U}^{1\cdot 2\cdots Q}$. We refer to this method as the Random Visit/Random RSS Sensing (RV/RS) method.

C. Random visits, tensor completion and random RSS sensing

Similar to the RV/RS method, we randomly select M voxels out of N_v voxels, but before selecting the data collection point, we reconstruct the RSS maps for all the TXs at all the voxels by means of a 3D tensor completion *as if UAV visits all the voxels.*

We define a 3D-RSS tensor in $\mathcal{R}$ for the q-th TX as

$$\mathbf{R}^q = \{R_{ijk}^q | \quad i = 1, 2, \cdots, N_1, \\ j = 1, 2, \cdots, N_2, k = 1, 2, \cdots, N_3\}. \tag{14}$$

Note that we can sense the RSSs at the voxels over the predetemined route Ω where UAV can receive the wireless signal from the q-th TX. Therefore, according to the Total Variation Low Rank Tensor Completion (TVLRTC) method [12], the reconstruction problem of a tensor $\mathbf{W}^q$ is given by ($q = 1, 2, \ldots, Q$)

$$\mathbf{W}^q = \{W_{ijk}^q | \quad i = 1, 2, \cdots, N_1, \\ j = 1, 2, \cdots, N_2, k = 1, 2, \cdots, N_3\} \tag{15}$$

$$\underset{\mathbf{W}^q}{\text{minimize}} \quad \lambda \sum_{n=1}^{3} \|\mathbf{F}_n \mathbf{W}_{(n)}^q\|_1 + (1-\lambda)\frac{1}{3}\sum_{n=1}^{3} \|\mathbf{W}_{(n)}^q\|_* \tag{16}$$

$$\text{subject to} \quad \mathbf{W}_{\Omega^q}^q = \mathbf{R}_{\Omega^q}^q. \tag{17}$$

In (16), $\|\mathbf{C}\|_1$ denotes the ℓ-1 norm of a matrix $\mathbf{C}$, that is, $\|\mathbf{C}\|_1 = \sum_o \sum_p |c_{op}|$, $\mathbf{F}_n = \{f_{op}\}$ is a smoothness constraint matrix, where

$$f_{op} = \begin{cases} 1 & (p = o) \\ -1 & (p = o+1) \\ 0 & (\text{otherwise}) \end{cases} \tag{18}$$

and $\mathbf{Q}_{(n)}$ denotes the mode-n unfolding matrix of $\mathbf{Q}$. Furthermore, $\|\mathbf{A}\|_* = \sum_m \sigma_m(\mathbf{A})$ denotes the nuclear norm of a matrix $\mathbf{A}$, where $\sigma_m(\mathbf{A})$ denotes the m-th largest singular value of $\mathbf{A}$. The first and second terms of (16) mean the total variation and low-rank tensor completion, respectively and λ is a tunable parameter to balance them. On the other hand, in (17), $(\cdot)|_{\Omega^q}$ is the operation of picking up the elements along the predetemined route Ω where UAV can receive the wireless signal from the q-th TX from $(\cdot)$. So finally, replacing the elements of $\mathbf{R}^q$ by those of $\mathbf{W}^q$, the problem is given by

$$\text{find} \quad \mathbf{U}_{\hat{m}} \in \mathcal{V} \tag{19}$$

$$\hat{m} = \arg_m \max \quad \{W_1^{min}, W_2^{min}, \ldots, W_{N_1N_2N_3}^{min}\}. \tag{20}$$

We refer to this method as the Random Visit/Tensor Completion/Random RSS sensing (RV/TC/RS) method.

V. Experiment and Performance evaluation

To evaluate the performance of the proposed method, we conducted an experiment in Osaka City University. Figure 2 (a) shows the photo of the experiment. We placed three TXs near the windows inside the buildings, which transmit the 2.4GHz band Wi-Fi signals, as shown in Figures 2 (b) - (d). On the other hand, the RSS sensing region had 3D sizes of $X = 30$m, $Y = 8$m and $Z = 10$m. The experimental site is located in an urban area, so flying a UAV in the air is prohibitive. Therefore, instead of UAV, we attached a receiver (RX) to the top of a pole, as shown in Figure 2 (e). Dividing the sensing region by 2m interval along the x-axis, y-axis, and z-axis, namely, $\Delta X = \Delta Y = \Delta Z = 2$m, $N_1 = 15$, $N_2 = 4$, and $N_3 = 5$, we sensed the RSSs for the TXs at each voxel in total $N_v = 300$ voxels. In addition, we set the RSS sensable probability $C_{rec} = 0.6$. TABLE I shows the specifications of experiment.

Figure 3 compares the fully sensed RSS map by the FV/FS method, the randomly selected RSS map by the RV/RS method

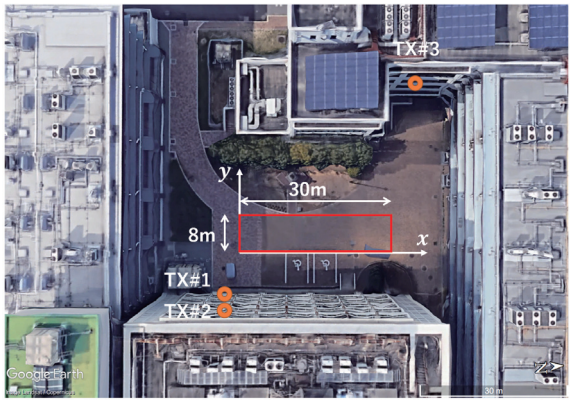

(a) Sensing region.

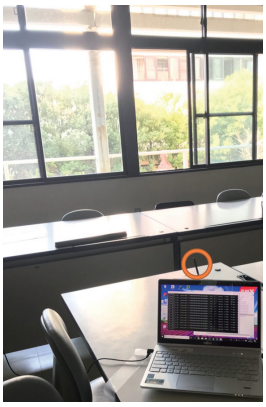

(b) TX#1.

(c) TX#2.

(d) TX#3.

(e) RX.

Figure 2. Photos of the experiment.

TABLE I. SPECIFICATIONS OF EXPERIMENT.

Location	Osaka City University
Sizes of sensing region	$X = 30\text{m} \times Y = 8\text{m} \times Z = 10\text{m}$
Sensing resolution	$\Delta X = \Delta Y = \Delta Z = 2$ m $N_1 = 15$, $N_2 = 4$, $N_3 = 4$, and $N_v = 300$
Number of TXs (Q)	3
Wireless communication tool	2.4GHz band Wi-Fi
Antenna	Dipole
RSS sensable probability	C_{rec}=0.6

and the reconstructed RSS map by the RV/TC/RS method, for the three TXs, respectively, when setting the RSS sensing ratio B_{sense} of 0.25 ($= 75/300$, $M = 75$) and $\lambda = 0.07$ [13]. Since the RSS sensable probability is set as $C_{rec} = 0.6$, the RSSs for TX#1, TX#2 and TX#3 are sensed only at 48 voxels, 43 voxels and 47 voxels out of 75 voxels, respectively, but we can see that the RSS maps can be accurately reconstructed by the tensor completion. Defining the Relative Square Error (RSE) of reconstructionfor the q-th TX as

$$\text{RSE}^q = \frac{||\mathbf{R}^q - \mathbf{W}^q||_F}{||\mathbf{R}^q||_F} \tag{21}$$

where $||(\cdot)||_F$ denotes the Frobenius norm of tensor $(\cdot)$, we obtain $\text{RSE}^1 = 0.06$, $\text{RSE}^2 = 0.03$, and $\text{RSE}^3 = 0.05$.

We have set $B_{sense} = 0.25$ and $\lambda = 0.07$ to show the RSS maps in Figure 3, but Figure 4 and Figure 5 show the dependencies of RSE^q on B_{sense} and λ, respectively. We can see that RSE^q becomes flat when B_{sense} is more than 0.2 and also it becomes flat when λ is more than 0.07.

Figure 6 compares the total route length among the FV/FS, RV/RS, and RV/TC/RS methods when setting $B_{sense} = 0.25$ and $\lambda = 0.07$. We can see that as compared with the FV/FS method, the RV/RS and the RV/TC/RS method can reduce the total route length by around 60%.

Finally, to compare the total data collection time among the three methods, according to the data sheet of Xbee Wi-Fi, we define $f(R^q_{\hat{m}})$ in Mbps as

$$f(R^q_{\hat{m}}) = \begin{cases} 6 & (-91 \le R^q_{\hat{m}} < -89) \\ 9 & (-89 \le R^q_{\hat{m}} < -88) \\ 12 & (-88 \le R^q_{\hat{m}} < -86) \\ 18 & (-86 \le R^q_{\hat{m}} < -83) \\ 24 & (-83 \le R^q_{\hat{m}} < -80) \\ 36 & (-80 \le R^q_{\hat{m}} < -76) \\ 48 & (-76 \le R^q_{\hat{m}} < -74) \\ 54 & (-74 \le R^q_{\hat{m}}) \end{cases}. \tag{22}$$

Figure 7 compares the total data collection time among the FV/FS, RV/RS, and RV/TC/RS methods for the case of $D^q = 100$MBytes (800×10^6 bits) ($q = 1, 2, 3$) when setting $B_{sense} = 0.25$ and $\lambda = 0.07$. The RV/RS method needs to select the best voxel out of fewer voxels (19 voxels) where the UAV happens to be able to sense the RSSs for all the

 ISBN: 978-1-61208-769-6

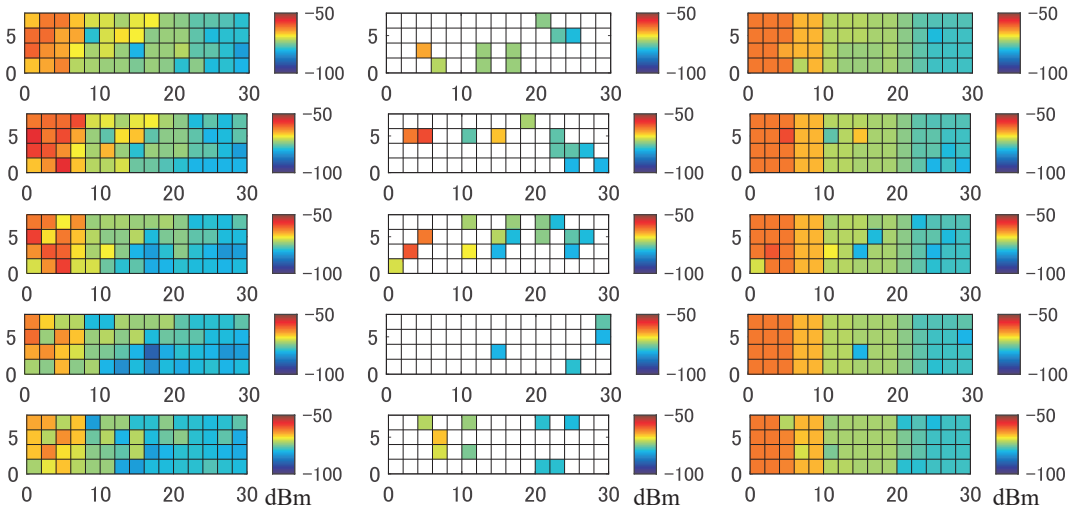

(i) FV/FS. (ii) RV/RS. (iii) RV/TC/RS.

(a) TX#1.

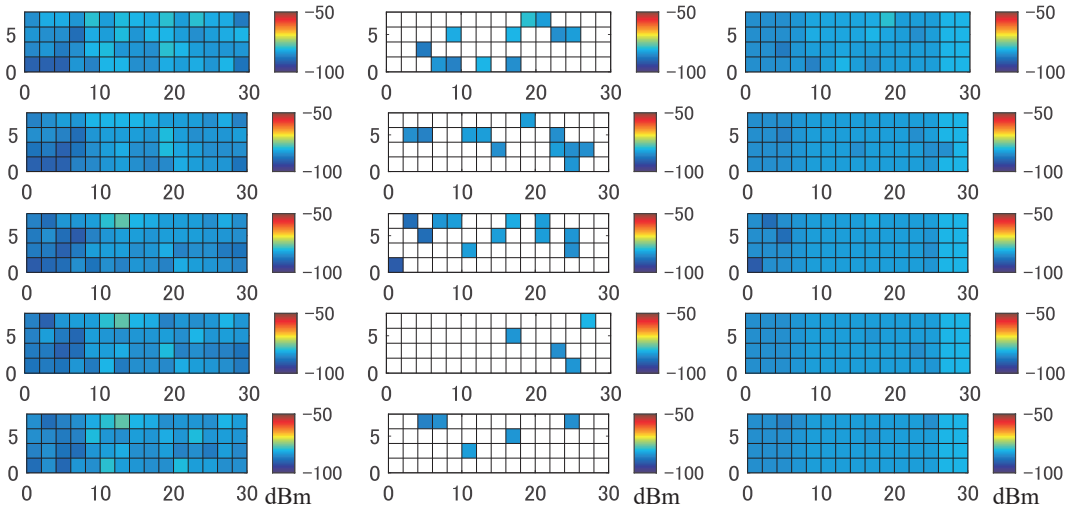

(i) FV/FS. (ii) RV/RS. (iii) RV/TC/RS.

(b) TX#2.

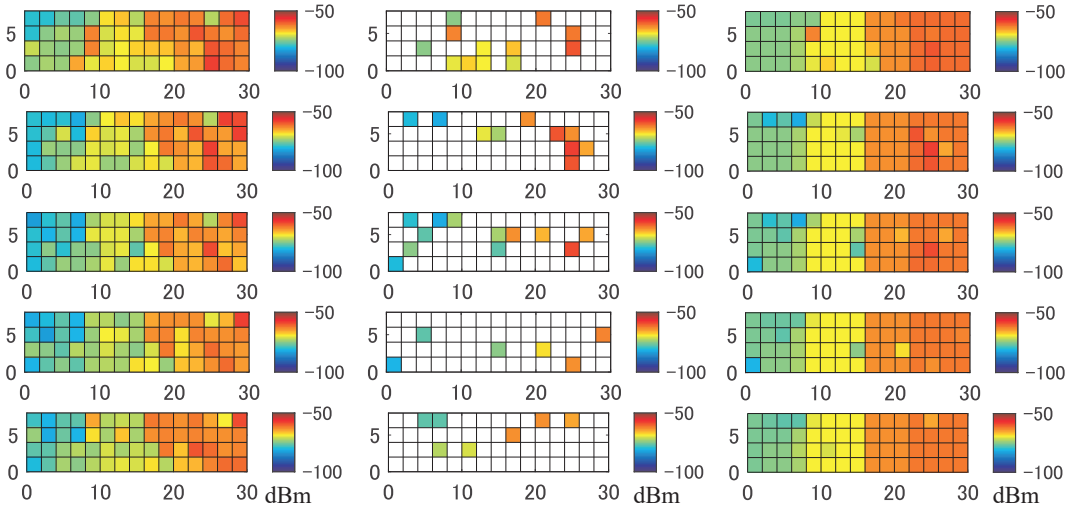

(i) FV/FS. (ii) RV/RS. (iii) RV/TC/RS.

(c) TX#3.

Figure 3. RSS maps ($B_{sense} = 0.25$, $\lambda = 0.07$).

 ISBN: 978-1-61208-769-6

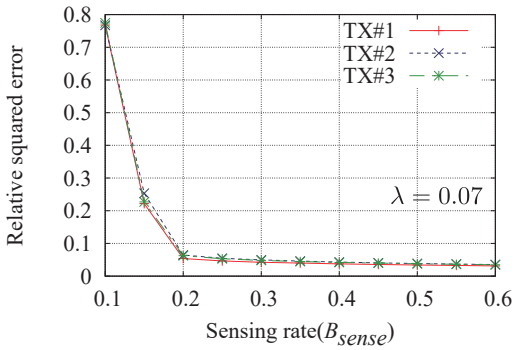

Figure 4. Dependency of the RSE on the RSS sensing rate (B_{sense}).

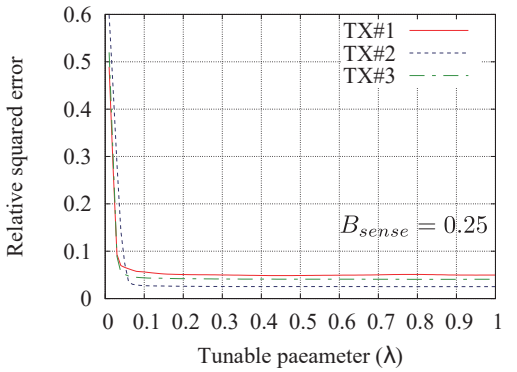

Figure 5. Dependency of the RSE on the tunable parameter (λ).

three TXs, so the selected voxels cannot give higher RSSs, resulting in a much longer data collection time. On the other hand, as the clue of the RSSs for the fewer selected voxels, the RV/TC/RS method can reconstruct the RSS maps for the three TXs almost perfectly through the tensor completion as if the UAV senses the RSSs fully in the entire 3D region. We can see that there is no difference in the total data collection time between the FV/FS method and the RV/TC/RS method.

VI. Conclusion and Future Work

In this paper, we have proposed the tensor completion-based method for selecting a single data collection point for multiple transmitters in a UAV-enabled disaster recovery network. The experimental results have shown that the RV/TC/RS method can select the truly best data collection giving the shortest data collection time by sensing the RSSs in 25% of the 3D region.

We have randomly selected a fewer RSS sensing points and simply connected them with a short route, so our future work includes the selection of RSS sensing points which can be connected with the shortest route while keeping the MAP reconstruction accuracy the highest. In addition, we have discussed a single data collection point selection, so another of our future works is to select multiple but less data collection points for multiple transmitters.

Acknowledgment

This study was supported in part by a Grant-in-Aid for Scientific Research (No. 18H01445) from the Ministry of Education, Science, Sport and Culture of Japan, and the ICOM Foundation, Japan.

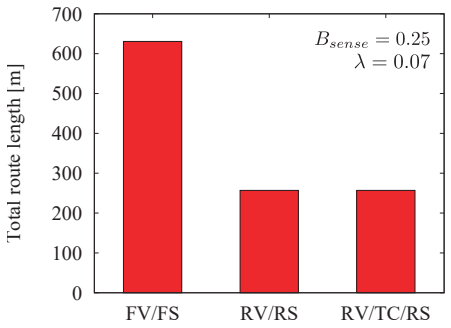

Figure 6. Total route length.

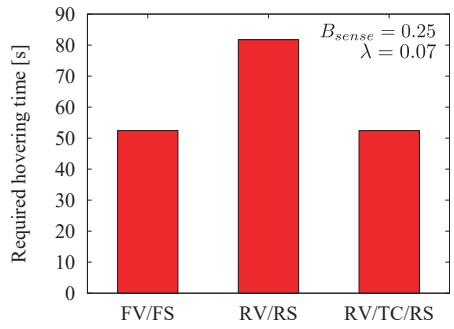

Figure 7. Total data collection time.

References

[1] A. M. Hayajneh, S. A. R. Zaidi, D. C. McLernon, M. Di Renzo, and M. Ghogho, "Performance analysis of UAV enabled disaster recovery networks: a stochastic geometric framework based on cluster processes," *IEEE Access*, vol. 6, pp. 26215-26230, May 2018.

[2] P. Toth and D. Vigo, *The Vehicle Routing Problem*, SIAM, 2002.

[3] M. Erdelj, E. Natalizio, K. R. Chowdhury and I. F. Akyildiz, "Help from the Sky: Leveraging UAVs for Disaster Management," *IEEE Pervasive Computing*, vol. 16, no. 1, pp. 24-32, Jan.-Mar. 2017.

[4] A. Vetrivel, M. Gerke, N. Kerle, F. Nex, G. Vosselman, "Disaster damage detection through synergistic use of deep learning and 3D point cloud features derived from very high resolution oblique aerial images, and multiple-kernel-learning," *ISPRS Journal of Photogrammetry and Remote Sensing*, vol. 140, pp. 45-59, 2018.

[5] J.Scherer, *et al.*, "An autonomous multi-UAV system for search and rescue," *Proc. ACM, First Workshop on Micro Aerial Vehicle Networks, Systems, and Applications for Civilian Use*, pp. 33-38, May 2015.

[6] K. Dorling, J. Heinrichs, G.G. Messier, and S. Magierowski, "Vehicle routing problems for drone delivery," *IEEE Trans. Syst., Man, Cybern. Syst.,* vol. 47, no.1, pp. 70-85, Jan. 2017.

[7] Wi-Fi Alliance, https://www.wi-fi.org/ [retrieved: Jan. 2020].

[8] C. Pei, *et al.*, "Why it takes so long to connect to a WiFi access point," *Proc. IEEE INFOCOM 2017*, pp. 1-9, May 2017.

[9] J. Y. Potvin, "Genetic algorithms for the traveling salesman problem," Annals of Operations Research vol. 63, pp. 339-370, June 1996.

[10] M. Dorigo and L.-M. Gambardella, "Ant colony system: a cooperative learning approach to the traveling salesman problem," *IEEE Trans. Evol. Comput.*, vol. 1, no. 1, pp. 53-66, Apr. 1997.

[11] IEEE Standard for Information technology Telecommunications and information exchange between systems Local and metropolitan area networks Specific requirements Part 11: Wireless LAN Medium Access Control (MAC) and Physical Layer (PHY) specifications Amendment 4: Further Higher Data Rate Extension in the 2.4 GHz Band, 2006.

[12] T.-Y. Ji, T.-Z. Huang, X.-L. Zhao, T.-H. Ma, and G. Liu, "Tensor completion using total variation and low-rank matrix factorization," Information Sciences, vol. 326, pp. 243-257, Jan. 2016.

[13] H. Nishioka *et al.*, "A compressed sensing-based 3D-RSS MAP completion for UAV routes planning," *Proc. ICST 2018*, pp. 273-277, Dec. 2018.

 ISBN: 978-1-61208-769-6